



## Short communication

## Measuring electrical components of lithium ion battery at different states of charge



K.H. Norian\*

Electrical and Computer Engineering Department, 19 Memorial Drive West, Lehigh University, Bethlehem, PA 18015, USA

## H I G H L I G H T S

- The equivalent circuit components of the lithium ion battery were measured.
- The 3.7 V 900 mA-hour capacity lithium ion battery was studied.
- Resistances varied from 0.01  $\Omega$  to 0.39  $\Omega$  and capacitances varied from 1.03 F to 16.23 F.
- The resistances were higher at 40% than at 100% state of charge.
- The capacitor decreased as the state of charge decreased.

## A R T I C L E I N F O

## Article history:

Received 22 December 2012

Received in revised form

27 May 2013

Accepted 28 May 2013

Available online 6 June 2013

## Keywords:

Lithium ion battery

Lithium battery components

Battery measurement method

Camera battery equivalent circuit

## A B S T R A C T

Equations that describe the voltage variations with time of rechargeable batteries during charging and discharging measurements are used to determine the component values of the equivalent circuit of lithium ion batteries as the battery state of charge (SOC) changes from 100% to 40% SOC. The battery is described as an ideal voltage source in series with a resistor and the parallel combination of a resistor and a capacitor. The model uses different values of resistance and capacitance, in the parallel combination, during the different phases of the discharge-rest-charge-rest sequence. For the 3.7 V 900 mA-hour camera battery resistances vary from 0.01  $\Omega$  to 0.39  $\Omega$  and capacitances from 1.03 F to 16.23 F. The resistances are higher at 40% SOC than at 100% SOC. For both the charge and discharge phases the capacitor value decreases as the SOC decreases. The component values are useful in the design of circuits driven by the lithium ion battery.

© 2013 Elsevier B.V. All rights reserved.

## 1. Introduction

The aim of this work was to determine the component values of the equivalent electric circuit of lithium ion (Li ion) batteries under different states of charge (SOC). The battery of interest was the nominal 3.7 V, 900 mA-hour capacity one. Rechargeable batteries usually find themselves in transient circuit applications where the design and performance evaluation of the circuit requires the equivalent circuit parameters of the battery under the charge, discharge and rest periods. Equivalent circuit parameters necessary for a precise transient analysis of circuits driven by the battery of interest were not available. In the present work typical values for equivalent component values for Li ion batteries at different states of charge are presented.

The most basic circuit of the battery is a voltage source in series with the internal resistance. The electrochemical processes

of rechargeable batteries [1,2] lead to a second, and more precise, equivalent circuit comprising a voltage source in series with a resistor and a parallel combination of a resistor and a capacitor [3–7]; the Thevenin model. The latter is used to model the battery under conditions of constant state of charge and constant temperature. This model is valid for discharge times of the order of seconds. This model was used in the present work together with a battery measurement method based on transient analysis. The method uses the discharge-rest-charge-rest sequence of the rechargeable battery with different values for the resistor and capacitor, in the parallel RC combination, for the charge and discharge phases and for the intervening rest periods. Equations for the temporal variation of the transient battery voltage were used to calculate the equivalent circuit components.

## 2. Theory

The equivalent circuit of the battery appears to the left of terminals *a* and *b* in Fig. 1 where  $v(t)$  is the battery voltage. It is a series

\* Fax: +1 610 758 6279.

E-mail address: [khn0@lehigh.edu](mailto:khn0@lehigh.edu).

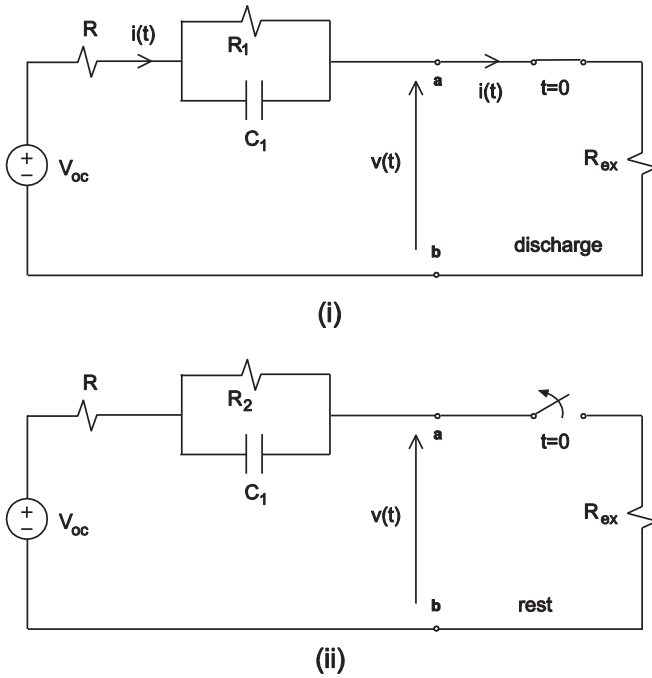


**Fig. 1.** The circuit for (i) the discharge period and (ii) the subsequent rest phase of the battery.  $v(t)$  is the battery voltage and  $R_{ex}$  is the external load resistor.  $V_{oc}$  is the open circuit voltage of the battery.  $R$  is the series resistance in the battery equivalent circuit.

combination of the open circuit battery voltage  $V_{oc}$ , a resistor  $R$ , and the equivalent of the parallel combination of a resistor and a capacitor.

Fig. 1(i) shows the battery equivalent circuit during the discharge phase.  $R_{ex}$  is the external resistor. Fig. 1(ii) shows the battery equivalent circuit in the rest period that follows the discharge phase. The capacitor value is  $C_1$  for both the discharge and the subsequent rest period, while  $R_1$  and  $R_2$  are the resistors in parallel with the capacitor in the discharge and rest periods, respectively.  $R$  represents the internal resistance of the battery. The capacitor and resistor in parallel represent the double layer capacitance and the resistance, respectively, of the electrode–electrolyte contact.

Fig. 2(i) shows the battery circuit during the charge phase.  $V_g$  is the charging voltage. The charge phase is followed by a rest period represented by Fig. 2(ii). The same battery model applies in the charge phase as in the discharge one but now with different values for the components in the parallel circuit. The capacitor value is  $C_2$  for both the charge and the subsequent rest period, while  $R_3$  and  $R_4$  are the resistors in parallel with the capacitor in the charge and rest periods, respectively. The series resistor  $R$  stays the same as in the discharge–rest case. The capacitor  $C_2$  and resistor in parallel ( $R_3$  or  $R_4$ ) represent the double layer capacitance and the resistance, respectively, of the electrode–electrolyte contact in the charge and subsequent rest periods. Since  $V_g > V_{oc}$  the voltage source  $V_g$  acts as a generator. The current  $i(t)$  flows into terminal  $a$  and ultimately into the positive terminal of  $V_{oc}$  as a charging current to the battery. The source  $V_{oc}$  now acts as the energy absorber.

Transients are involved during the charging and discharging of batteries. Abrupt changes are recorded in the voltage across the terminals of the battery as the switch is closed or opened at the start of these transients. These boundary value changes in voltage as well as voltage levels in the intervening transients are used here to calculate circuit parameters. The temporal variation of the voltage across the battery terminals during the discharge–rest–charge–rest sequence appears in Fig. 3. The equations for the

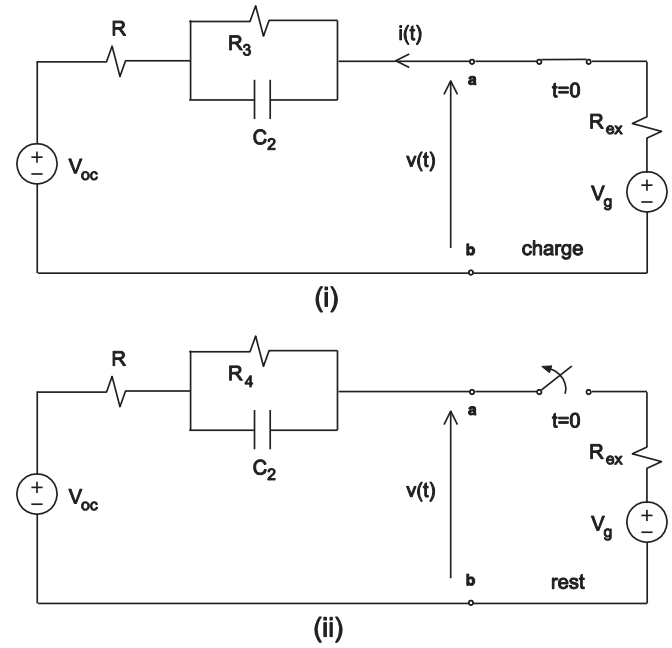


**Fig. 2.** The equivalent circuit for the battery in (i) the charging phase followed by (ii) the resting period.  $V_g$  is the external charging voltage.  $V_g > V_{oc}$ .

variation in the battery voltage  $v(t)$  during the discharge–rest–charge–rest sequence were derived earlier [8,9] and so are given here without derivation. These equations correspond to the voltage levels  $V_1$  to  $V_7$  that are shown in Fig. 3 and are relevant to the measurement technique. The equations that were used to calculate the equivalent circuit parameters of the Li ion battery are

$$R = R_{ex} \left( \frac{V_{oc}}{V_2} - 1 \right) \quad (1)$$

$$R_1 = R \left( \frac{V_{oc}}{V_4 - V_3} - 1 \right) - R_{ex} \quad (2)$$

$$R_2 = \frac{R_1 V_{oc}}{(R + R_1 + R_{ex}) C_1 \left( \frac{dv}{dt} \right)_{r1}} \quad (3)$$

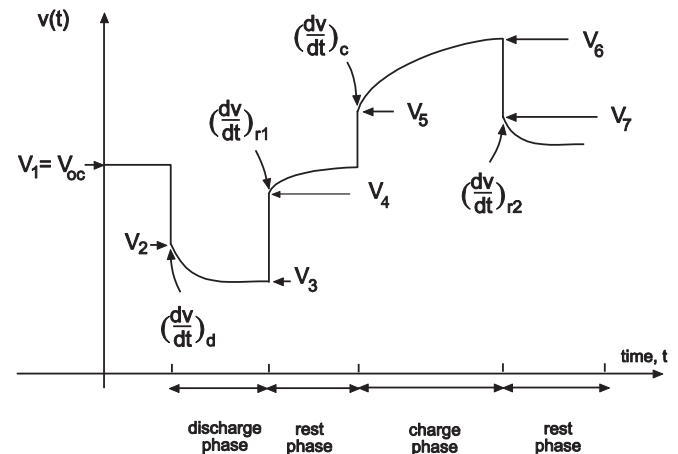


**Fig. 3.** The battery terminal voltage  $v(t)$  as a function of time during the discharge and rest phases, followed by the charge and rest phases showing the voltage levels  $V_1$  to  $V_7$ .

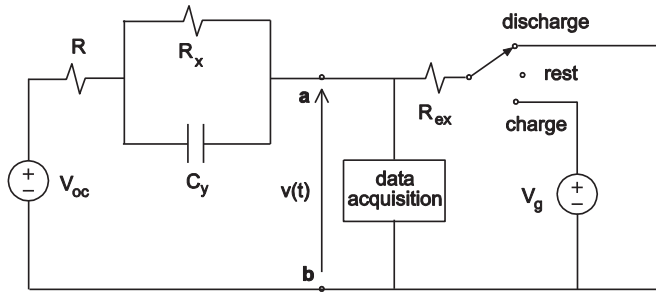


Fig. 4. The circuit used for measuring the temporal variation of the battery voltage during the discharge–rest–charge–rest phases.

Table 1

Component values of the equivalent circuit of three Li ion batteries of equal capacity at states of charge of 40%, 70% and 100%.

SOC	40%	70%	100%
(i)			
$R$	0.39 $\Omega$	0.28 $\Omega$	0.32 $\Omega$
$R_1$	0.07 $\Omega$	0.01 $\Omega$	0.02 $\Omega$
$R_2$	0.07 $\Omega$	0.01 $\Omega$	0.02 $\Omega$
$C_1$	1.04 F	7.99 F	10.91 F
$R_3$	0.08 $\Omega$	0.02 $\Omega$	0.03 $\Omega$
$R_4$	0.10 $\Omega$	0.03 $\Omega$	0.03 $\Omega$
$C_2$	1.03 F	4.95 F	12.41 F
(ii)			
$R$	0.28 $\Omega$	0.25 $\Omega$	0.23 $\Omega$
$R_1$	0.03 $\Omega$	0.01 $\Omega$	0.01 $\Omega$
$R_2$	0.03 $\Omega$	0.01 $\Omega$	0.01 $\Omega$
$C_1$	2.25 F	8.56 F	10.54 F
$R_3$	0.05 $\Omega$	0.03 $\Omega$	0.04 $\Omega$
$R_4$	0.06 $\Omega$	0.03 $\Omega$	0.04 $\Omega$
$C_2$	2.66 F	13.75 F	15.07 F
(iii)			
$R$	0.30 $\Omega$	0.24 $\Omega$	0.23 $\Omega$
$R_1$	0.09 $\Omega$	0.01 $\Omega$	0.01 $\Omega$
$R_2$	0.09 $\Omega$	0.01 $\Omega$	0.01 $\Omega$
$C_1$	3.57 F	12.52 F	15.29 F
$R_3$	0.12 $\Omega$	0.02 $\Omega$	0.02 $\Omega$
$R_4$	0.13 $\Omega$	0.03 $\Omega$	0.02 $\Omega$
$C_2$	3.06 F	11.83 F	16.23 F

$$C_1 = \frac{R_{ex} V_{oc}}{(R + R_{ex})^2 \left( \frac{dv}{dt} \right)_d} \quad (4)$$

$$R_3 = R \left( \frac{V_g - V_{oc}}{V_6 - V_7} - 1 \right) - R_{ex} \quad (5)$$

$$R_4 = \frac{R_3 (V_g - V_{oc})}{(R + R_3 + R_{ex}) C_2 \left( \frac{dv}{dt} \right)_{r2}} \quad (6)$$

$$C_2 = \frac{R_{ex} (V_g - V_{oc})}{(R + R_{ex})^2 \left( \frac{dv}{dt} \right)_c} \quad (7)$$

where the respective gradients at the start of the discharge phase and at the start of the subsequent rest period are  $(dv/dt)_d$  and  $(dv/dt)_{r1}$ , respectively, while the respective gradients at the start of the charge phase and at the start of the subsequent rest period are given by  $(dv/dt)_c$  and  $(dv/dt)_{r2}$ .

### 3. Results and discussion

Li ion batteries nominally rated at 3.7 V, and a 10 h capacity of 900 m-Ah were examined. The discharge–rest–charge–rest curve of a fully charged battery was first obtained. The battery was then discharged to 70% SOC and then to 40% SOC and the discharge–rest–charge–rest curve at each SOC was recorded. Each curve was a plot of the battery voltage  $v(t)$  as a function of time and was recorded with

the battery at room temperature. Fig. 4 shows the circuit used for measuring the discharge–rest–charge–rest curve. A single pole double throw switch with center off was used to switch between phases and the resulting temporal variation in the battery voltage was recorded by connecting the data acquisition probe between terminals *a* and *b*. Fig. 5 shows the discharge–rest–charge–rest curve of a battery at 40% SOC.

The charging voltage  $V_g$  during the charge phase was 4.80 V. The external load resistor  $R_{ex}$  was 10  $\Omega$ . The open circuit battery voltage  $V_{oc}$  was 3.53 V, 3.76 V and 4.08 V at 40%, 70% and 100% SOC, respectively.

The battery displayed large abrupt voltage changes at the beginning of each phase in its discharge–rest–charge–rest curve. These changes in  $v(t)$  were then followed by transients of short duration where the battery voltage recovered to a steady state value within seconds.

Circuit components could be calculated to within  $\pm 0.01$ . The component values of the equivalent circuit of three batteries are given in Table 1. Resistances vary from 0.01  $\Omega$  to 0.39  $\Omega$  and

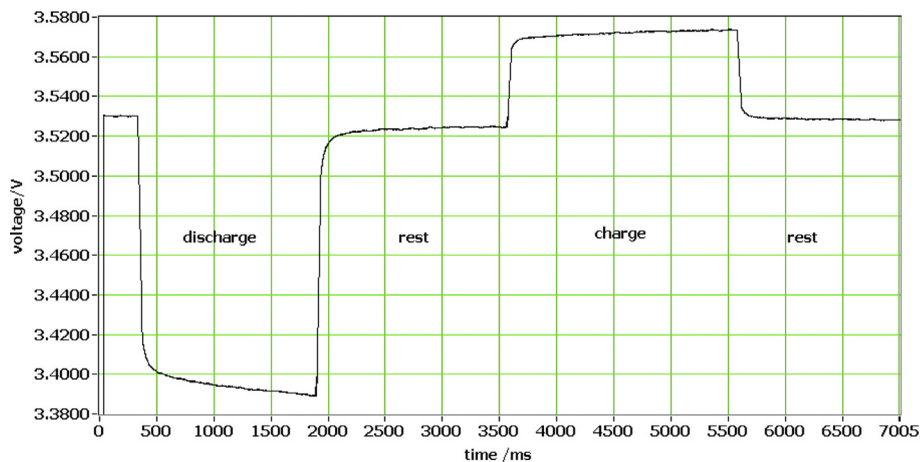


Fig. 5. The temporal variation of the battery voltage  $v(t)$  in the discharge–rest–charge–rest characteristics of a Li ion battery at a state of charge of 40%.

capacitances from 1.03 F to 16.23 F. The equivalent circuit resistances increase and capacitances decrease as the SOC decreases. For the battery of Table 1(i)  $R$ ,  $R_1$ ,  $R_3$  increase from 0.32  $\Omega$ , 0.02  $\Omega$ , 0.03  $\Omega$  to 0.39  $\Omega$ , 0.07  $\Omega$ , 0.08  $\Omega$ , respectively and  $C_1$ ,  $C_2$  decrease from 10.91 F, 12.41 F to 1.04 F, 1.03 F, respectively as SOC decreases from 100% to 40%. The increase in  $R$ , representing the internal resistance of the battery, indicates the decrease in the density of ions for electrical conduction as SOC decreases. The increase in  $R_1$  and  $R_3$  (the resistance of the double layer at the electrode-electrolyte contact) and the decrease in  $C_1$  and  $C_2$  (the capacitance of double layer at the electrode-electrolyte contact) mean that, since resistance is directly proportional to and capacitance is inversely proportional to the thickness of the double layer, then during both discharging and charging, the thickness of the double layer at the electrode–electrolyte contact increases as the SOC decreases.

The order of magnitude decrease in capacitance between the two extremes of SOC makes the capacitor in the parallel RC circuit a good indicator of the battery SOC.

#### 4. Conclusions

Equations that describe the voltage variations with time of rechargeable batteries during charging and discharging, and in the

boundary regions between these phases, were used to determine the component specifications of the equivalent circuit of lithium ion batteries under different states of charge. For the 3.7 V, 900 mA-hour battery resistances varied from 0.01  $\Omega$  to 0.39  $\Omega$  and capacitances from 1.03 F to 16.23 F. The resistances were higher at 40% SOC than at 100% SOC. For both the charge and discharge phases the capacitor value decreased as the SOC decreased. The value of the capacitor in the parallel resistor–capacitor circuit is an indicator of the battery SOC. The component values would be useful in the design of circuits driven by the lithium ion battery.

#### References

- [1] H. Bode, *Lead Acid Batteries*, John Wiley, New York, 1977.
- [2] M.A. Dasoyan, I.A. Aguf, *Current Theory of Lead Acid Batteries*, Technicopy Ltd., England, 1979.
- [3] Z.M. Salameh, M.A. Casacca, W.A. Lynch, *IEEE Transactions on Energy Conversion* 7 (1) (1992) 93–98.
- [4] M.A. Casacca, Z.M. Salameh, *IEEE Transactions on Energy Conversion* 7 (3) (1992) 442–446.
- [5] H.L. Chan, D. Sutanto, in: *IEEE Power Engineering Society Winter Meeting*, vol. 1, 2000, pp. 470–475. Singapore.
- [6] W.A. Lynch, Z.M. Salameh, in: *IEEE Power Engineering Soc. Meeting, Montréal* (2006), paper no. 06GM1201.
- [7] S.R. Nelatury, P. Singh, *Journal of Power Sources* 112 (2002) 621–625.
- [8] K.H. Norian, *Journal of Power Sources* 196 (2011) 2360–2363.
- [9] K.H. Norian, *Journal of Power Sources* 196 (2011) 5205–5208.